**Research Article***Copyright © All rights are reserved by Yohichi Kohzuki*

Study on Thermal Activation Barrier for Dislocation Motion by Strain-Rate Cycling Tests Combined with Ultrasonic Oscillations

Yohichi Kohzuki**Department of Mechanical Engineering, Saitama Institute of Technology, Japan*

***Corresponding author:** Yohichi Kohzuki, Department of Mechanical Engineering, Saitama Institute of Technology, 1690 Fusaiji, Fukaya, Saitama 369-0293, Japan.

Received Date: October 12, 2022**Published Date: October 20, 2022****Abstract**

The strain-rate cycling tests between two strain-rates of $1.1 \times 10^{-5} \text{ s}^{-1}$ and $5.5 \times 10^{-5} \text{ s}^{-1}$ in the middle of ultrasonic oscillatory stress were conducted during the plastic deformation of NaBr:Li⁺ (0.5 mol%) single crystals at 77 to 263 K. This method is considered to give the effective stress τ_p , when a dislocation begins to overcome the isotropic defects produced around the additive ions (Li⁺) in the ionic crystal with the help of thermal activation. Then, the τ_p -temperature relationship is fitted to the Cottrell-Bilby model within the temperature by numerical calculation with the parameters: τ_p value (1.08 MPa) at 0 K, T_c (469 K) and G_0 (0.50 eV) for the ionic crystal. T_c is the critical temperature at which τ_p is zero. G_0 is the activation energy for the dislocation motion.

Keywords: Dislocation; Isotropic defects; Plastic deformation; Ultrasonic oscillation; Strain rates

Introduction

It is well known that a dislocation will encounter a stress field illustrated schematically in Figure 1 as it moves through on the slip plane containing many weak obstacles and a few strong ones [1,2]. In the figure, the positive stress concerning axis of the ordinate opposes the flow stress (applied stress), τ , and the negative stress assists it. Extrinsic resistance to the dislocation motion has two types: one is long-range obstacle (the order of 10 atomic diameters or greater) and the other short-range obstacle (less than about 10 atomic diameters). The former is considered to be forest dislocations, large precipitates or second-phase particles, and grain

boundary, for instance, and the latter impurity atoms, isolated and clustered point defects, small precipitates, intersecting dislocations, etc. Overcoming the latter type of obstacles (byname, thermal obstacles) by a dislocation, thermal fluctuations play an important role in aid of the flow stress above the temperature of 0 K. As both resistances simultaneously act on a dislocation, the flow stress τ consists of two components: an internal stress τ_i (athermal component) due to the long-range obstacles and an effective stress τ^* due to short-range ones (thermal component). τ is given by the following Equation 1, since τ^* depends on temperature T and strain rate $\dot{\epsilon}$ [3, 4].

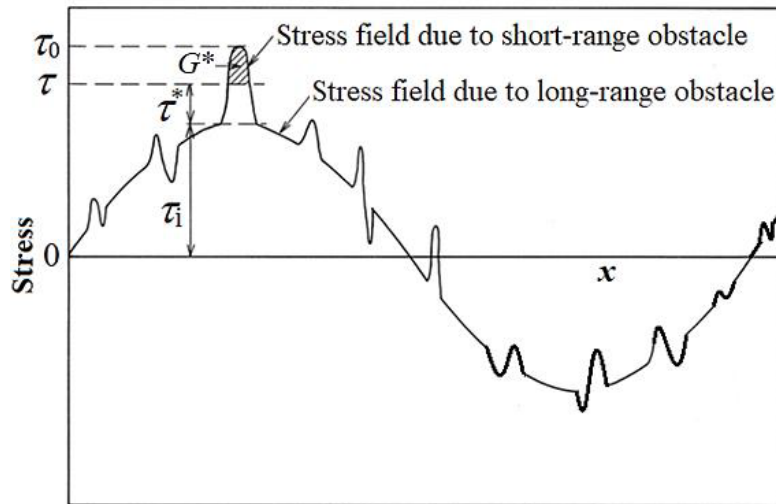


Figure 1: Stress fields encountered by a dislocation moving through the crystal lattice.

$$\tau = \tau^*(T, \dot{\epsilon}) + \tau_i \tag{1}$$

Then the aid energy, G^* , supplied by the thermal fluctuations is given by the shaded part in Figure 1. Thus, the dislocation can move through below τ_0 . τ_0 is the value of τ at 0 K. As for the long-range obstacles (byname, athermal obstacles), the energy barrier is so large that the thermal fluctuations play no role in overcoming them within the temperature.

The representation of Figure 2 is concerned with a common type of thermal activation barrier. The free energy (G) varies with the distance (x) between a dislocation and the obstacle as given in Figure 2(a). When a dislocation overcomes the short-range obstacles, the free energy becomes high on account of the work (W) done

by the applied stress. Then the resistance (F), where it can be defined by the differentiation of free energy with respect to x (i.e., $\partial G^*/\partial x$), to the dislocation motion is revealed as Figure 2(b) in accord with the abscissa of Figure 2(a). Figure 2(b) corresponds to the typical force-distance curve for the short-range obstacle among those in Figure 1. Shape of this curve represented by $F(x)$ means the model overcoming the obstacle by a dislocation. G_0 , which is taken as the shaded area under $F(x)$ in Figure 2(b), is the Gibbs free energy of activation for the breakaway of a dislocation from the obstacle in the absence of an applied stress (in this case it is equivalent to the Helmholtz free energy for the dislocation motion). G^* in Figure 1 corresponds to the difference between G_0 and W ($W = \int_{x_0}^{x_2} \tau^* b L dx$), namely,

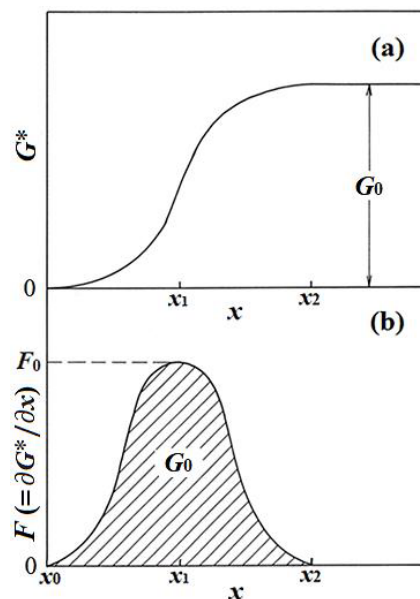


Figure 2: The process for thermal activated overcoming of the short-range obstacle by a dislocation. Variation in (a) the Gibbs free energy of activation and (b) the force acted on the dislocation with the distance x for a dislocation motion.

$$G^* = G_0 - W = 2 \int_{x_1}^{x_2} \{F(x) - \tau^* bL\} dx, \quad (F(x_1) = F_0, x_2 > x_1) \quad (2)$$

where b is the magnitude of the Burgers vector, L is the average length of dislocation segments, x_0 and x_2 are the values of x at which F equals the defect force, and F_0 is the maximum value of F (i.e., F at the distance x_1).

Results and Discussion

The strain-rate cycling tests associated with ultrasonic oscillation (20 kHz) were carried out during plastic deformation for NaBr single crystals doped with Li^+ ions. The concentration of the dopant ions was 0.5 mol% in melt. Figure 3 shows the experimental results on $\Delta\tau$ vs. λ for the crystals at various temperatures and a given strain. The numbers besides each symbol in the figure represent the temperature of the crystal. $\Delta\tau$ is the stress drop due to super-

position of ultrasonic oscillatory stress. λ ($\lambda = \Delta\tau' / \Delta \ln \dot{\epsilon}$) is the strain-rate sensitivity of flow stress and was obtained from the stress change ($\Delta\tau'$) due to the strain-rate cycling between the two strain rates (1.1×10^{-5} and $5.5 \times 10^{-5} \text{ s}^{-1}$) in the middle of ultrasonic oscillatory stress [5,6]. The relative curves have stair like shape below 263 K in Figure 3 [7]. The $\Delta\tau$ value at first bending point is termed τ_p , as denoted in Figure 3. The value of τ_p becomes smaller at higher temperature and disappears at 263 K. Because it has been reported for other crystals that its value depends on temperature and impurity concentration [8,9], the τ_p is considered to represent the effective stress due to the dopant ions which lie on the dislocation when a dislocation begins to overcome the defects produced around the dopants with the help of thermal activation during plastic deformation. The plots in Figure 4 represent τ_p for NaBr: Li^+ single crystals at 77 to 263 K.

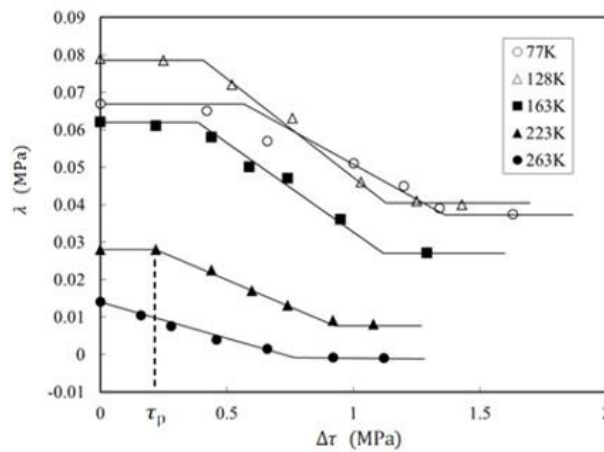


Figure 3: Stress decrement ($\Delta\tau$) vs. λ for NaBr: Li^+ (0.5 mol%) at 77 to 263 K [7].

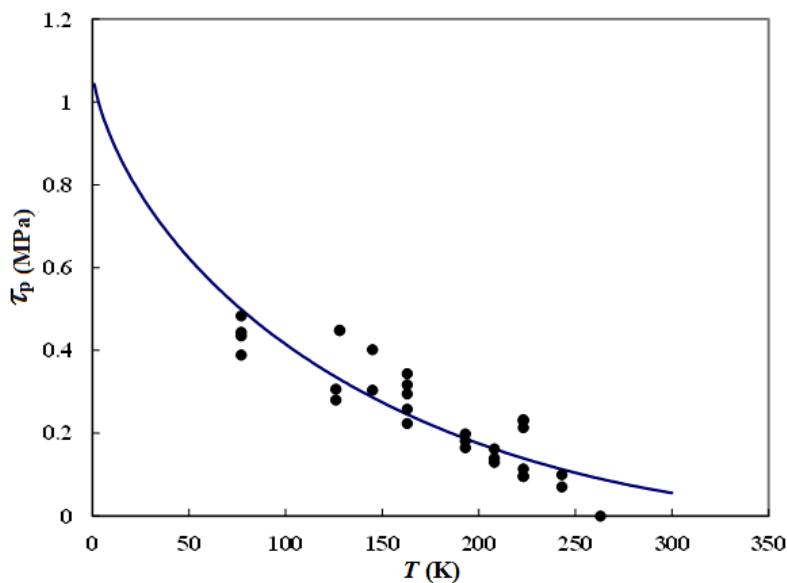


Figure 4: Dependence of τ_p on temperature for NaBr: Li^+ (0.5 mol%).

Isotropic defects occur around them in NaBr single crystals doped with monovalent ions, since their size is different from the substitutional ions (Na^+) of the host crystal. The force-distance profile between a dislocation and the symmetry defect is expressed by the Cottrell and Bilby relation [10] taking account of the Friedel relation [11]. As a function of the distance x along the slip plane away from the obstacle by ρ , the force F interacting between a dislocation and an obstacle is given by [10]

$$F = \frac{2G_0\rho x}{(x^2 + \rho^2)^{3/2}} \quad (3)$$

where F is maximum at $x = \rho/\sqrt{3}$. The relation between the effective stress and temperature for NaBr:Li⁺ (0.5 mol%) crystal is exhibited as the solid curve in Figure 4, where is determined by numerical calculation with the parameters: τ_{p0} , T_c and G_0 (0.50eV). τ_{p0} (1.08 MPa) is the value of τ_p at the temperature of 0 K. T_c (469 K) is the critical temperature at which τ_p is zero. Figure 4 shows that the curve agree with the τ_p data (i.e., solid circles in the figure), which is based on $\Delta\tau$ vs. λ at a given strain (see Figure 3), within the temperature.

Conclusion

Overcoming the isotropic defects around the dopants (Li^+) in NaBr:Li⁺ crystal by a dislocation with the help of thermal activation during plastic deformation, the effective stress τ_p becomes smaller and smaller with the temperature below 263 K. The temperature dependence of τ_p is approximated to the Cottrell-Bilby relation. Then, the parameters are estimated to be τ_{p0} (1.08 MPa), T_c (469 K) and G_0 (0.50 eV) for the ionic crystal.

Acknowledgement

None.

Conflict of Interest

No conflict of interest.

References

1. Conrad H (1964) Thermally activated deformation of metals. *Journal of Metals* 16: 582-588.
2. Messerschmidt U (2010) *Dislocation Dynamics During Plastic Deformation*. Berlin Heidelberg: Springer, pp.180-187.
3. Sprackling MT (1976) *The Plastic Deformation of Simple Ionic Crystals*. Academic Press, London, pp.128-129.
4. Argon AS (2008) *Strengthening Mechanisms in Crystal Plasticity*. Oxford University Press Inc., New York, pp.106-108.
5. Kohzuki Y, Ohgaku T (2016) I⁻ ions as obstacles to dislocation motion in NaCl:I⁻ single crystals. *Journal of Materials Science and Chemical Engineering* 4: 1-8.
6. Kohzuki Y (2018) Study on dislocation-dopant ions interaction in ionic crystals by the strain-rate cycling test during the Blaha effect. *Crystals* 8(1): 31-54.
7. Kohzuki Y, Ohgaku T (2017) Study on influence of additive and host ions on deformation characteristics of alkali halide crystals by strain-rate cycling tests during the Blaha effect. *Crystal Research and Technology* 52(3): 1600290.
8. Ohgaku T, Teraji H (2001) Investigation of interaction between a dislocation and a Br⁻ ion in NaCl:Br⁻ single crystals. *Physica Status Solidi (a)* 187(2): 407-413.
9. Ohgaku T, Matsunaga T (2009) Interaction between dislocation and divalent impurity in KBr single crystals. *IOP Conference Series: Materials Science and Engineering* 3: 012021.
10. Cottrell AH, Bilby BA (1949) Dislocation theory of yielding and strain ageing of iron. *Proceedings of the Physical Society of London A* 62: 49-62.
11. Friedel J (1964) *Dislocations*. Pergamon Press, Oxford, pp. 223-226.